Al-Azhar Bull. Sci. Vol. 19, No. 1 (June.): pp. 153-167, 2008.

ELECTROCHEMICAL BEHAVIOR OF STEEL ALLOYS AS AFFECTED BY PHOSPHORIC ACID

A. S. I. AHMED*, R. M. ABOU SHAHBA*, IBRAHIME M. GHAYAD**, E. M. ATTIA* AND W. A. M. HUSSEIN*

**Chemistry Department, Faculty of Science (for Girls), AL- Azhar University, Nasr City, Cairo, Egypt*

***Central metallurgical research and development institute*

Abstract

The behavior of two steel alloys in phosphoric acid solutions alone and with addition of organic and inorganic compounds was studied using open circuit potential and potentiodynamic polarization techniques. Open circuit potential measurements of the two stainless steel electrodes in different concentrations of H_3PO_4 showed that the rates of film thickening of the two electrodes are independent of the solution concentration. Potentiodynamic polarizations illustrate that, upon increasing Na_3PO_4 concentration in 0.5M H_3PO_4 the pH of the solutions changed in the range from 1.7 to 10.7 and the corrosion rate decreases. Electrode type (II) has inhibition efficiency more than electrode type (I). AT compound (3 amino 1, 2, 4-triazole) has proven to be efficient inhibitor for pitting corrosion of stainless steel in phosphoric acid solutions. The inhibition efficiency was increased by increasing the inhibitor concentration. The inhibitive property may be argued to the formation of a compact Fe-AT complex film on the electrode surface.

Introduction

Stainless steels are selected as engineering materials mainly because of their excellent corrosion resistance. Small amounts of chromium, about 5%, add some corrosion resistance to iron, but in order to make stainless steel "stainless", at least 12% Cr is required. Addition of nickel to stainless steels improves their corrosion resistance in neutral or weakly oxidizing media [1, 2]. Molybdenum forms a passive MoO_2 film in the active region of stainless steels and hence decreases the active dissolution current [3]. In order to achieve improved pitting corrosion resistance, Mo content should be higher than 1%. The best results are obtained for alloys with Mo content between 3% and 4% [4]. Duplex and super duplex stainless steels are used in applications in media containing ions from the halogen family, mainly the chloride ion [5,6] and have good sea water corrosion resistance [2,7]. The corrosion rate of some stainless steel alloys in industrial phosphoric acid increases with the increase of temperature. Alloys which contain chromium, molybdenum and nitrogen in sufficient quantities present the best behavior [8].

Many authors have studied the corrosion of steels with its different alloys and their inhibition by organic inhibitors in acid solutions [9-14]. Organic molecules are used to inhibit corrosion of steel alloys [15-21]. Among most of organic compounds, heterocyclic substance containing nitrogen atoms, such as triazole-type compounds is considered to be excellent corrosion inhibitor for many metals and alloys in various aggressive media [22-25].

It is hoped that this work may showed some light on the corrosion behavior of two types of electrodes with different chemical composition in phosphoric acid solutions. Also, the corrosion inhibition of stainless steels by (4-57%) sodium phosphate and (1-2%) AT (3 amino 1, 2, 4-triazole) in 0.5 M phosphoric acid was investigated.

Experimental

Two electrodes of stainless steel alloys with chemical composition are given in Table (1). Cylindrical electrodes with a working surface area of 0.68 cm^2 were used. Electrodes were enclosed in a holder which can be made in contact with the test solution. Before use, the electrodes were ground with emery paper and polished with diamond paste (1μm), finally the samples were cleaned by bi-distilled water and ethyl alcohol, and then quickly inserted in the cell. The complete wetting of the electrode surface upon wash was taken as a criterion for the cleanness of the surface.

Analytical grade reagents were used in all experiments with bi-distilled water.

Table (1): Chemical composition of the two types of electrodes

Samples	Amount of Elements (%)					
	Si	**Cr**	**Mn**	**Fe**	**Ni**	**Mo**
Electrode (I)	1.27	18.72	1.86	70.65	5.05	2.45
Electrode (II)	0.56	17.28	1.14	67.83	10.57	2.62

Open-circuit potential measurements were carried out in a conventional glass cell of 150ml solution. The potentials were measured with respect to an external saturated calomel electrode (SCE) interfaced to the test solution via a salt bridge. The potential measurements were carried out using electronic multimeter (Type: Escord EDM-2116).

Potentiodynamic polarization measurements were performed on Autolab GPES 30 (General Purpose Electronically System, Eco Chemie B.V., Utrecht, the Netherlands). An electrochemical cell with a standard working electrode and platinum sheet as an auxiliary electrode and Ag/AgCl as reference electrode was used.

A potentiodynamic current-potential curves were recorded using a scanning rate of 1mV/sec. between -450 up to 1000 mV. All measurements were performed in freshly prepared solutions at room temperature (25±2^{o}C).

Results and Discussion

1. Open – circuit potential measurements of stainless steel electrodes in aqueous phosphoric acid media:

Figures (1,2) represent the variation of the steady state potential($E_{s.s}$) of the two stainless steel electrodes type (I and II) with time in solutions of different concentrations(0.05-5.0M) of phosphoric acid. The open circuit potentials of the two electrodes have always a general tendency for steady state potential to shift steadily towards nobler values with decreasing acid concentrations; this is indicative of film formation and thickening with decreasing acid concentrations.

The potential-time curves of stainless steel electrodes type (I and II) in H_3PO_4 solutions show that, stable passivity is possible under a range of conditions, the transition to the active state being favored by increasing acid concentrations. For this application, anodic protection is required to maintain a passive state, which would otherwise undergo a periodic breakdown [26-28]. In spite of the successful application of anodic protection, a consensus is yet to be attained on the nature of the passive state of stainless steels in this concentrated acid solution.

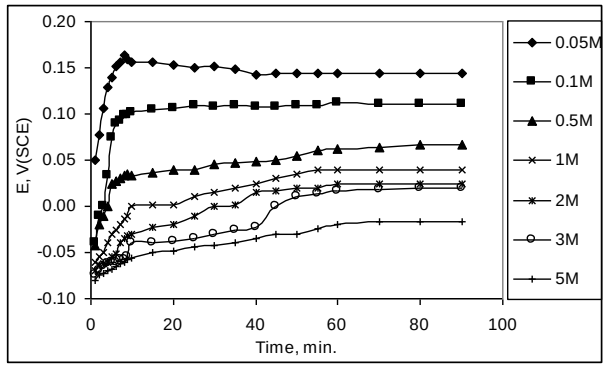

Figure (1): Potential – time curves of electrode (I) in different concentrations of H_3PO_4 acid.

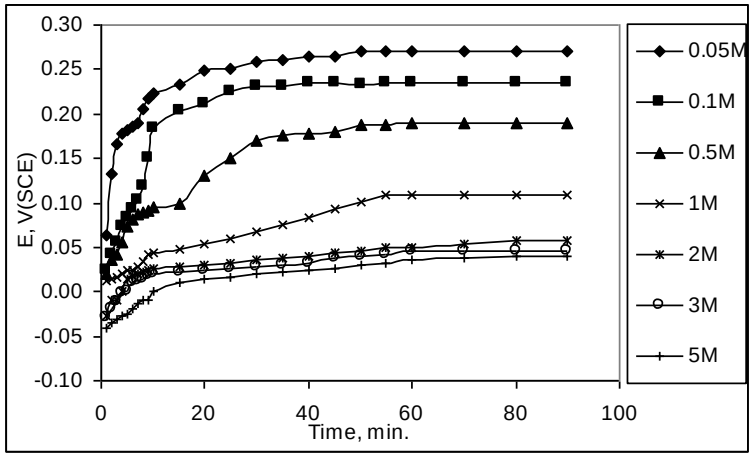

Figure (2): Potential – time curves of electrode (II) in different concentrations of H_3PO_4 acid.

The immersions as well as the steady state potential values for all concentrations in stainless steel electrodes seem to fall in Fe_2O_3 region of the Pourbaix diagram [29]. The general shift to noble direction points toward oxidation of Fe_3O_4 to Fe_2O_3. The high positive shift indicates the high amount of Fe_2O_3 present in the oxide layer.

$$4Fe_3O_4 + 2H_2O = 6Fe_2O_3 + 4H^+ + 4e^-$$
$$4e^- + O_2 + 2H_2O = 4OH^-$$
$$4Fe_3O_4 + O_2 = 6Fe_2O_3$$

The variation of steady-state potential ($E_{s.s}$) of the two steel electrodes with the logarithm of the molar concentration, C, of the acid solutions, is represented in figure (3). $E_{s.s}$ varies linearly with log C according to equation:

$$E_{s.s} = a_1 - b_1 \log C$$

Where a_1 and b_1 are constants depending on the type of solution: "a_1" represents the steady state potential, $E_{s.s}$, in solution of 1.0M concentration, as obtained from the lines making the best fit with experimental results. Values of "a_1" are 0.07V and 0.16V for electrodes type I and II, respectively.

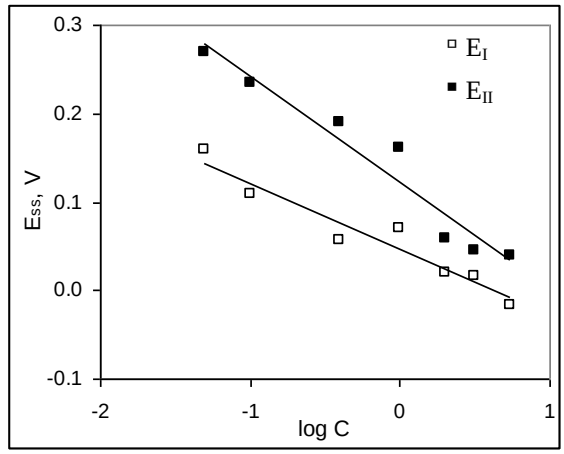

Figure (3): E_{ss}/log C of electrodes I and II in different concentrations of H_3PO_4 solutions.

By presenting the data in the form of potential - log time curves, straight lines were obtained (figures 4,5) satisfying the relation [30]:

$$E = \text{constant} + 0.039\ (\delta)\ \log t$$

Where: t is the time from the moment of immersion in solution and δ is the rate of oxide film thickening per unit decade of time.

Potential of the two examined electrodes varies linearly with the logarithm of the immersion time until $E_{s.s}$ is attained. From the slopes of the linear portions of the straight lines one readily calculates values of δ for the two stainless steel electrodes examined. The values of δ thus obtained are listed in Table (2).

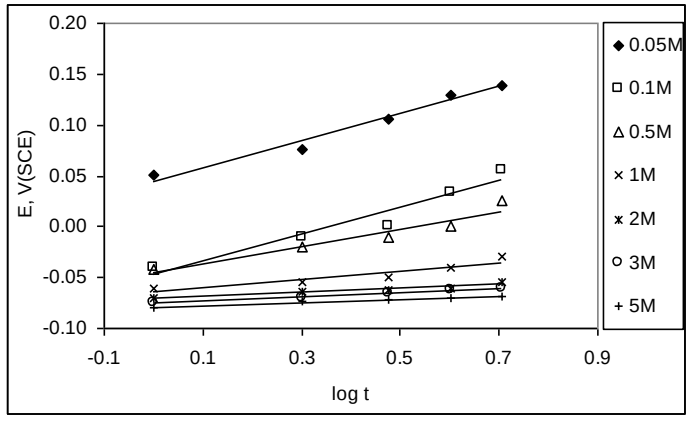

Figure (4): Potential/log C relations of electrode I in different concentrations of H_3PO_4 solutions.

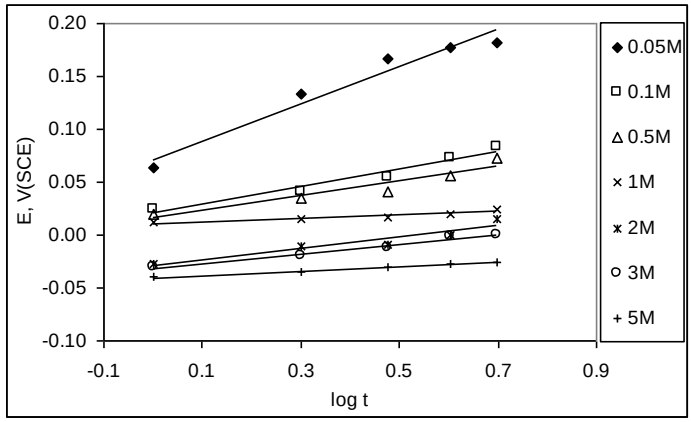

Figure (5): Potential/log t relations of electrode II in different concentrations of H_3PO_4 solutions.

Table (2): Rates of film thickening δ (nm / decade of time) of electrodes (I) and (II) in H_3PO_4 acid solutions

Conc., M	δE_I	δE_{II}
0.05	3.382	4.443
0.10	3.338	2.118
0.50	2.190	1.777
1.00	1.024	0.405
2.00	0.517	1.377
3.00	0.536	1.157
5.00	0.423	0.539

Consideration of the data included in Table (2), the rates of film thickening of stainless steel electrodes are independent of the solution concentration.

2. Potentiodynamic polarization Measurements

2.1. Stainless steel electrodes in phosphoric acid solutions:

The potentiodynamic polarization curves of the two test electrodes type (I) and (II) in phosphoric acid solutions at 25^0C are shown in figures (6,7). The electrochemical parameters of the test electrodes type I and II, corrosion potential ($E_{corr.}$), corrosion current density ($I_{corr.}$), corrosion rate (C.R.), anodic (B_a) and cathodic (B_c) Tafel slopes are tabulated in Table (3).

From Table (3), for electrodes type (I) and (II), the corrosion potential values become more negative while corrosion current density values become more anodic and the corrosion rate increased as the concentration of H_3PO_4 solutions increased from 0.05 to 5.0M. Also, it is observed that anodic Tafel slope values, for electrodes

type I and II is decreased as the concentration is increased. Cathodic Tafel values are independent on concentration.

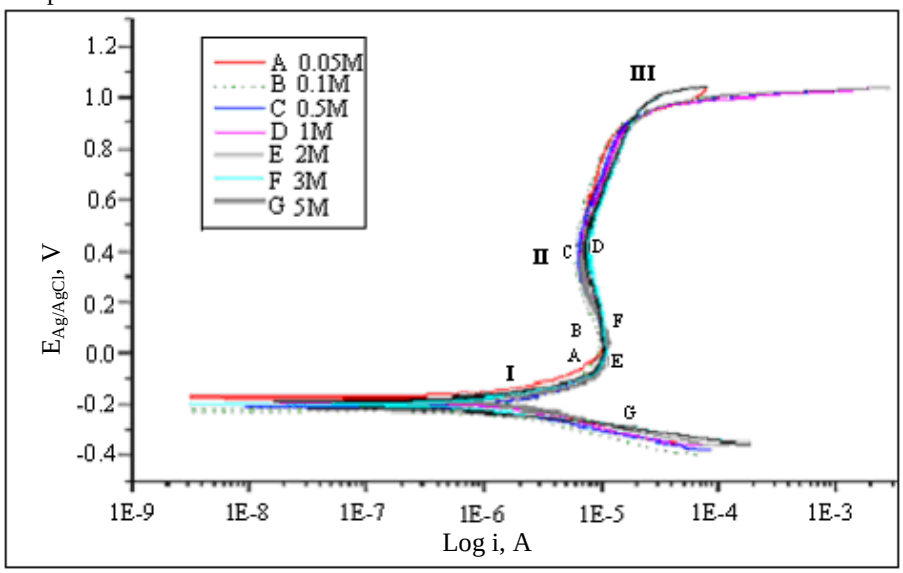

Figure (6): Anodic and cathodic polarization curves of electrode type (I) in (0.05 – 5M) phosphoric acid solutions.

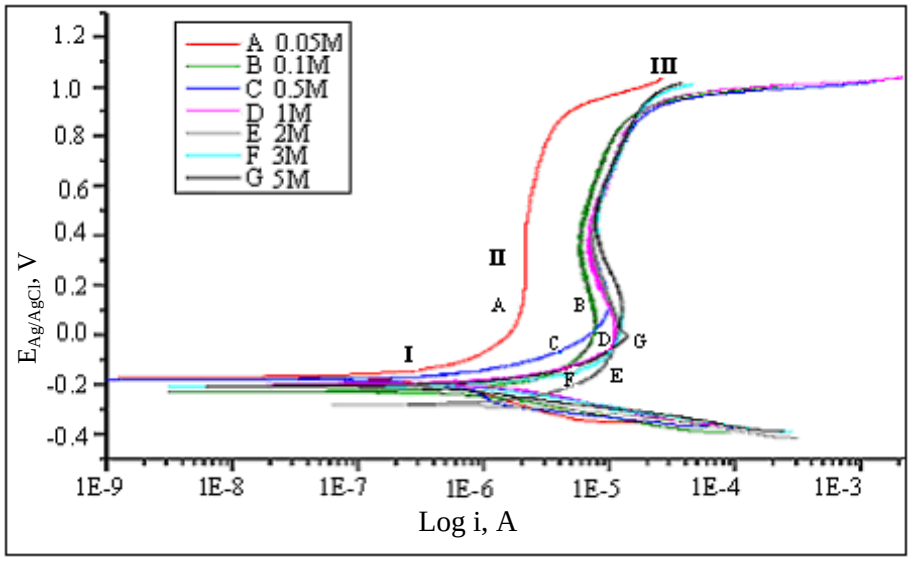

Figure (7): Anodic and cathodic polarization curves of electrode type (II) in (0.05 – 5M) phosphoric acid solutions.

Table (3): electrochemical parameters of electrodes I and II in H_3PO_4 solutions.

Alloy Type	Conc., M	$E_{corr.}$ V	B_a V/decade	B_c V/decade	$I_{corr.}$ A/cm^2	C.R. mm/year
(I)	0.05	-0.173	0.189	0.1116	6.142E-7	1.119E-2
	0.10	-0.222	0.188	0.1115	8.977E-7	1.613E-2
	0.50	-0.212	0.163	0.1370	1.379E-6	2.478E-2
	1.00	-.0191	0.160	0.1400	2.211E-6	4.221E-2
	2.00	-0.196	0.159	0.1400	2.871E-6	4.614E-2
	3.00	-0.224	0.150	1.3940	1.341E-5	8.122E-2
	5.00	-0.228	0.145	1.3320	2.551E-5	1.255E-1
(II)	0.05	-0.165	0.236	0.1554	2.686E-7	4.825E-3
	0.10	-0.227	0.206	0.1540	4.315E-7	5.263E-3
	0.50	-0.176	0.146	0.1022	9.797E-7	1.760E-2
	1.00	-0.189	0.132	0.1441	9.947E-7	1.816E-2
	2.00	-0.279	0.109	0.1221	0.874E-6	1.814E-2
	3.00	-0.284	0.091	0.1072	1.062E-6	1.907E-2
	5.00	-0.285	0.051	0.0944	2.224E-6	0.947E-1

Potentiodynamic behavior show that the cathodic current density is due to the hydrogen evolution. On the other hand, the anodic curves indicated three regions. The first region (I), active dissolution region was observed from -450 to -100 and to -175 $mV_{Ag/AgCl}$ where the potential-current relations were linear with a well defined Tafel slope. The second region (II), a current peak signifying the transition from active dissolution to passive state on electrode surface, from -50 to 800, zero to 850$mV_{Ag/AgCl}$. In the third region (III), a transpassive potential is observed at 850 to 1000, 950 to 1100$mV_{Ag/AgCl}$. Oxygen started to evolve and the current density increased sharply with further increase in potential. Increasing the acid concentration shift the active-passive transition potential and passive-transpassive transition potential regions toward the active direction.

The composition of the passive film of stainless steel electrodes formed in (0.05-5.0M) H_3PO_4 solution essentially composes from mixture of ferric phosphate, chromium phosphate and Fe_2O_3 [(31)]. The most interesting feature of film composition from stainless steel containing Mo is the existence of low amount of oxidized iron and phosphate together with remarkable enrichment in hexavalent Mo and trivalent chromium. This suggests the passive effect of chromium is reinforced probably by the formation of silico-molybdic compounds stable at the acid concentrations studied.

Finally, the passive film of the Mo containing stainless steels shows an enrichment in Mo(VI), Si(IV) and Cr(III), and a small amount of phosphate and

oxidized iron[32]. It is found that the improved corrosion behavior is directly correlated to its enrichment in silicon and molybdenum, and with depletion in iron in the surface film. This suggests that the protective properties of the passive film on Mo-stainless steel are correlated to the formation of silico-molybdic-hydrate compounds. In the active range, Mo dissolves in an oxidized state Mo(III), which are oxidized into MoO_4^{2-} or $HMoO_4^-$. They are stable in the concentrations of H_3PO_4 acid examined and then are adsorbed in the alloy surface and interact with various species, giving both mixed phosphate of Fe, Cr, Mo and simple phosphate $[H_3(PMo_{12}O_{40})]$[33]. Moreover, there is the probable appearance of silico-molybdic-hydrate complex that provides enough protection. The principle of these should be $H_4(12MoO_3,SiO_2).nH_2O$ particularly stable in acidic solutions[34].

2.2. Effect of addition of sodium phosphate on 0.5M H_3PO_4 acid solutions

Anodic and cathodic curves were generated potentiodynamically in figures (8,9) to investigate the effect of tri-basic sodium phosphate, Na_3PO_4, dosage (4-57%) on the corrosion behavior of the same electrodes in 0.5M H_3PO_4 solution. The electrochemical parameters in absence and presence of different concentrations of the additive are given in Table (4).

It was found that, upon increasing Na_3PO_4 concentration in the used acid solution, the corrosion current ($I_{corr.}$) decreases and the corrosion rate decreases; furthermore the pH of the solution changed in the range from 1.7 to 10.7. Therefore the protective property of additive depends on the pH value of the solution.

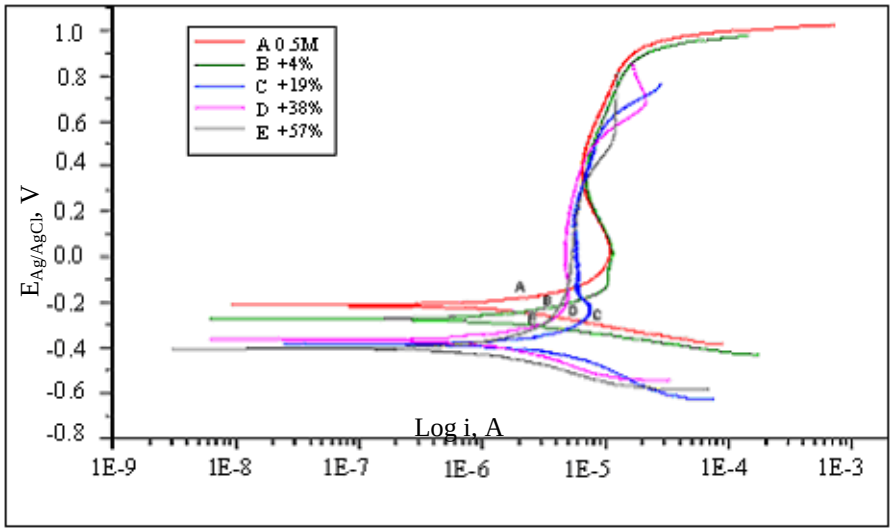

Figure (8): Anodic and cathodic polarization curves of electrode type (I) in 0.5M phosphoric acid with (4 – 57 %) Na_3PO_4 solutions.

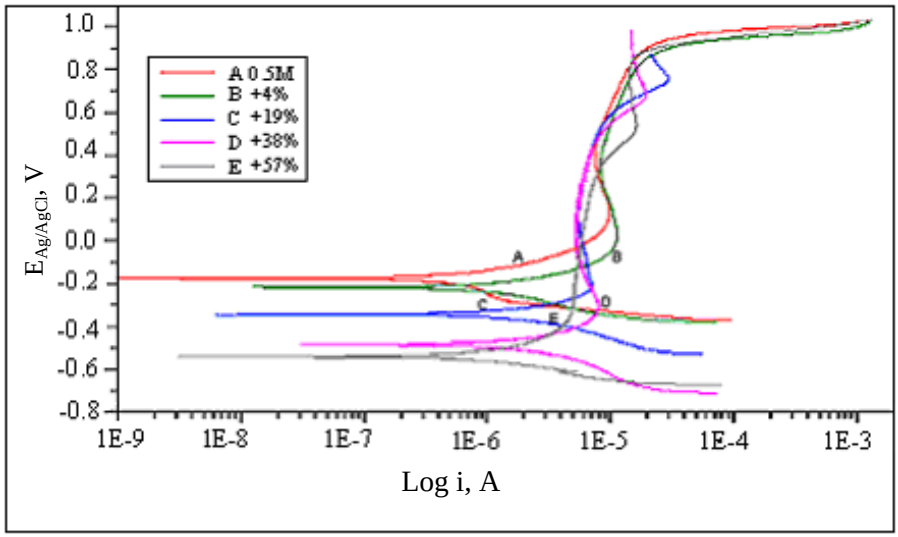

Figure (9): Anodic and cathodic polarization curves of electrode type (II) in 0.5M phosphoric acid with (4 – 57 %) Na_3PO_4 solutions.

The slopes of the anodic and cathodic Tafel lines (B_a and B_c) almost changed upon increasing the concentration of phosphate. This indicates that the used inhibitor has an effect on the mechanism of the dissolution of the used steel electrodes.

Table (4): Corrosion parameters and inhibition efficiencies, (I.E %) of the two electrodes in 0.5M H_3PO_4 with (4-57%) sodium phosphate.

Alloy Type	Na_3PO_4 %	$E_{corr.}$ V	Tafel Slopes B_a	Tafel Slopes B_c	$I_{corr.}$ A/cm^2	C.R. mm/year	(I.E %)
(I)	0	-0.212	0.163	0.137	1.379E-6	2.478E-2	--
	4	-0.251	0.151	0.136	1.211E-6	1.047E-2	12.183
	19	-0.383	0.125	0.136	8.139E-7	9.911E-3	40.979
	38	-0.387	0.120	0.135	5.079E-7	9.023E-3	63.169
	57	-0.401	0.055	0.107	2.128E-7	7.547E-3	84.569
(II)	0	-0.176	0.146	0.102	9.797E-7	1.76E-2	--
	4	-0.227	0.075	0.103	4.061E-7	7.295E-3	58.549
	19	-0.342	0.065	0.100	1.152E-7	3.121E-3	88.241
	38	-0.478	0.061	0.099	9.92E-8	1.782E-3	89.874
	57	-0.538	0.055	0.074	5.31E-8	5.121E-4	94.580

The behavior of stainless steel electrodes type (I) and (II) in HPO_4^{2-} ion solutions exhibited an active – passive behavior. The polarization measurements were

performed from the cathodic potential through the active and passive regions. At the beginning of the curve at a potential of -600 $mV_{Ag/AgCl}$, the electrode is activated. The positive change in potential causes an increase in dissolution rate for the stainless steel electrodes. Following this, the anodic current increases slightly with a rise in potential till value of approximately 900 $mV_{Ag/AgCl}$ at which the electrode becomes passive, forming a protective film on the electrode surface. This protective film consists of δ-Fe_2O_3 with $FePO_4.H_2O$ particles imbedded in it [35,36]. The high corrosion resistance of steel in phosphates solutions is undoubtedly due to the formation of sparingly soluble salts, and it can serve as an illustration of the specific effect of the anion [35].

From the results obtained, it can be concluded that the analysis of the experimental data in a phosphate medium of pH values from 1.7 to 10.7, allowed proposing a dissolution-precipitation mechanism type in order to interpret the presence of the first anodic peak and its evolution in relation with the experimental parameters studied. Phosphate ions are consumed, through a control by diffusion towards the interface, leading to a decrease of electrode active surface which is caused by precipitation of the oxidized iron species. The second peak is due to oxide formation rather than precipitation [37,38]. It is also clear that the inhibition effect of phosphate is due to the partial passivation of the electrode exerts on indirect effect of the cathodic reaction, increasing its rate, and will the anodic reaction retard. It is also found that electrode type (II) is more affected than electrode type (I), the high efficiency is 94.6% in 57% concentration for electrode type (II) and is 84.6% in the same concentration of solution for electrode type (I).

2.3. Effect of addition of 3-amino 1, 2, 4-triazole (AT) on the electrochemical behavior of stainless steel electrodes in phosphoric acid solutions:

Organic corrosion inhibitors function by chemisorptions of their molecules on metallic substrate, complexing of the molecules with metal ions that remain in solid lattices, neutralizing the corrodent and/or absorbing the corrodent. Many organic compounds containing polar group and π-electrons are good corrosion inhibitors for steels [39,40].

Curves of figures (10,11) show the variation of electrode potential with current density in solutions of 0.5M phosphoric acid in absence and presence of ascending concentrations of AT (1-4%). The results of the electrochemical parameters obtained indicate that, upon increasing the AT concentration, the values of $E_{corr.}$, $I_{corr.}$, Tafel slopes (B_a, B_c), and corrosion rate decrease (Table 5).

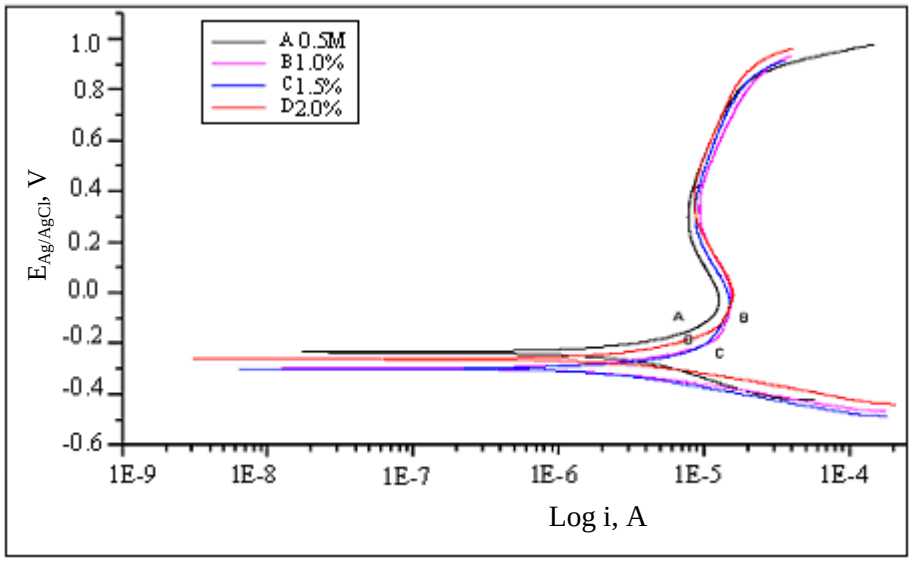

Figure (10): Anodic and cathodic polarization curves of electrode type (I) in 0.5M phosphoric acid with (1– 2 %) AT solutions.

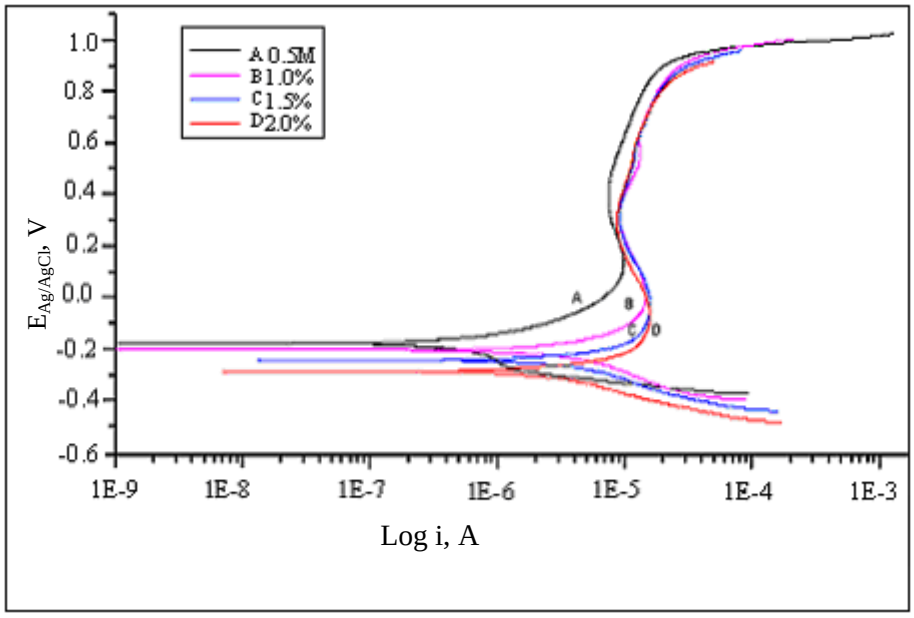

Figure (11): Anodic and cathodic polarization curves of electrode type (II) in 0.5M phosphoric acid with (1– 2 %) AT solutions.

Table (5): The corrosion parameters and inhibition efficiency, (I.E %) of Electrode I and II in 0.5M H_3PO_4 with AT inhibitor

Alloy type	*AT %*	$E_{corr.}$ *V*	Tafel Slopes B_a	Tafel Slopes B_c	$I_{corr.}$ A/cm^2	C.R mm/year	(I.E %)
(I)	0.0	-0.212	0.163	0.137	1.379E-6	2.478E-2	--
	1.0	-0.259	0.138	0.092	1.344E-6	2.415E-2	2.538
	1.5	-0.298	0.087	0.097	1.098E-6	1.972E-2	20.377
	2.0	-0.299	0.057	0.096	3.156E-7	5.669E-3	77.114
(II)	0.0	-0.176	0.146	0.102	9.797E-7	1.760E-2	--
	1.0	-0.203	0.101	0.101	9.744E-7	1.446E-2	0.541
	1.5	-0.242	0.083	0.045	8.051E-7	1.110E-2	17.822
	2.0	-0.286	0.055	0.093	6.179E-7	1.750E-3	36.930

Inhibitive effect of AT compound was related to the formation of a physical barrier on the electrode surface due to molecules adsorption and film formation [(41)]. From the experimental results, it is known that the inhibitive properties of 3-amino 1, 2, 4-tiazole depend mainly on the electron densities around the adsorption center and molecular size. However, the results of inhibition efficiency (I.E%) showed that, it increases by increasing the inhibitor concentration (Table 5). These results suggest that, when AT is present in acid solution, the oxide film is mainly composed of Fe_2O_3. But by increasing the concentration of AT, the surface film may be essentially an organic film. The inhibitive property may be argued to the formation of very low soluble layer and a compact Fe-AT complex film on the electrode surface [(39,40)]. Also, it is clear that the efficiency of AT in phosphoric acid solutions for stainless steel type I is varied from that obtained for the electrode type II. This variation of inhibition effect may be due to the change in the composition of the two electrodes especially in the nickel percentage, which increases probability of dissolution of the complex layer formed at the electrode surface.

Conclusion

The passive film formed in H_3PO_4 solution consists of mixture of $CrPO_4$, $FePO_4$ and Fe_2O_3. In phosphate solution, electrode type II has inhibition efficiency more than electrode type I due to the higher Cr, Ni and Mo contents. The high corrosion resistance of steel in phosphate solutions is due to the formation of sparingly soluble salts. AT compound has proven to be efficient inhibitor for pitting corrosion of stainless steel in H_3PO_4 acid solutions. Inhibitive effect of AT compound was related

to the formation of a physical barrier on the electrode surface due to molecules adsorption and film formation.

References

1. Anon; Advanced Materials and Processes, 154(4), pp.63, (1998).
2. F. William and Smith; Structure And Properties of Engineering Alloys, Mcgraw-Hill,Inc., 2nd Edition, Chapter 7, (1993).
3. K. Hashimoto, K. Asami, A. Kawashima, H. Habazaki and E. Akiyama; Corro. Sci., 49, pp. 42, (2007).
4. R. A. Merello, F. J. Botanab, J. A. Botella, M. V. A. Matres, M. b. Marcos, and S. A. Acerinox; Corro. Sci., 45, pp. 909, (2003).
5. M. Martins and L.C. Casteletti; Materials Characterization, 55(3), pp. 225, (2005).
6. Gustaf Back and Preet, M. Singh; Corro. Sci., 46, pp. 2159, (2004).
7. L.L. Shreir; "Corrosion, Metal / Environment Reaction", Butterworths, 1, pp. 3, (1977).
8. G. Abdellah, M. A. Hajji, J. El Miloudi and A. Ben Bachir; App. Surf. Sci., 253(5), pp. 2362, (2006).
9. Q. Ling-Guang, X. An-Jian, S. Yu-Hua; Mater. Chem. Phys., 91, pp. 269, (2005).
10. G. Quartarone, L. Bonaldo and C. Tortato; App. Surf. Sci., 252(23), pp.8251, (2006).
11. A. Tizpar and Z. Ghasemi; App. Surf. Sci., 252(24), pp. 8630, (2006).
12. D. John , A. Blom, S. Bailey, A. Nelson, J. Schulz, R. De Marco and B. Kinsella; Physica B, 385–386, pp. 924, (2006).
13. M.A. Deyab; Corros. Sci., 49, pp. 2315, (2007).
14. Q. Ling-Guang , Y. Wu, W. Yi-Min and X. Jiang; Corros. Sci., 50, pp. 576, (2008).
15. F. Bentiss, M. Traisnel and M. Lagrenée; Corros. Sci., 42, pp. 127, (2000).
16. A. Chetouani, A. Aouniti, B. Hammouti, N. Benchat, T. Benhadda and S. Kertit; Corros. Sci., 45, pp.1675, (2003).
17. M. Lagrenée, B. Mernari, N. Chaibi, M. Traisnel, H. Vezin and F. Bentiss; Corros. Sci., 43, pp.951, (2001).
18. S.S. Abd El-rehim, S. A. M. Refaey, F. Taha, M.B. Saleh and R.A. Ahmed; J. App. Electrochem., 31, pp. 429, (2001).
19. F. Bentiss, M. Traisnel, N. Chaibi, B. Mernari, H. Vezin and M. Lagrenée; Corros. Sci., 44, pp.2271, (2002).
20. K. Tebbji, H. Oudda, B. Hammouti, M. Benkaddour, M. El Kodadi, F. Malek and A. Ramdani; App. Surf. Sci., 241, pp.326, (2005).

21. M. Bouklah, A. Attayibat, S. Kertit, A. Ramdani and B. Hammouti; App. Surf. Sci., 242, pp.399, (2005).

22. M.A. Quraishi and H.K. Sharma; Mater. Chem. Phys., 78, pp. 18, (2002).

23. D. Chebabe, Z.A. Chikh, N. Hajjaji, A.A. Srhiri and F. Zucchi; Corros. Sci., 45, pp.309, (2003).

24. F. Bentiss, M. Traisnel, L. Gengembre and M. Lagren´ee; App. Surf. Sci., 161, pp. 194, (2000).

25. F. Bentiss, M. Lagrenee, M. Traisnel and J.C. Hornez; Corros. Sci., 41, pp. 789, (1999).

26. Y.S. Chang; Active Passive Corrosion Behavior, Ph.D. Dissertation, Cambridge University, Cambridge, (1984).

27. R. Matsuhashi, H. Abe, S. Abe and H. Kihira; Corro. Engin., 36, pp. 531,(1987).

28. J. R. Kish, M. B. Ives and J. R. Roddaba; Materials Sci. Forum, (185-188), pp. 887, (1995).

29. M. Pourbaix; Atlas of Electrochemical Equilibrium in Aqueous Solutions, Pergamon Press, Oxford, pp. 308-311, (1966).

30. J. M. Abd EL Kader and A. M Shams El Din; Br. Corros. J., 14 (1), pp. 40, (1979).

31. G. Lewis, P. G. Fox and P. J. Boden; Corro. Sci., 20, pp. 331, (1980).

32. T. N. Rhodin; Corros., 12, pp. 465, (1956).

33. J. P. Lee; Corros., 37, pp. 467, (1981).

34. A. Guenbour, J. Faucheu and A. Ben Bachir; Corro. Houston, 44 (4), pp. 214, (1988).

35. U.R. Evans; An Introduction to Metallic Corrosion, Edwared Arnold, London, (1960).

36. I. L. Rozefeld; Corrosion Inhibitors, Mc Grraw-Hill. Inc, 175,(1981).

37. B.E. Conway and D.C. W. Kannangara; J. Electrochem. Soc., 134, pp. 906, (1987).

38. J. Benzakour and A. Derja; Electrochim. Acta, 38, pp. 2547, (1993).

39. A.M. Badawi, S.T. Keera and M.A. Hussein; J. Egypt. Petro., 10 (2), pp. 25, (2001).

40. T. Giordano; Chemical Industries, 28, Corrosion Mechanism, Florian M.M.D., Ed., Marcel Dekker, UK (1987).

41. S. Muralidharan, M.A. Quraishi and S.V.K. Lyer; Corro. Sci., 37, pp. 1739, (1995).